JOURNAL OF MATERIALS SCIENCE 19 (1984) 2519–2532

Micromechanisms of crack initiation in thin films and thick sections of polyethylene

SWAPAN K. BHATTACHARYA, NORMAN BROWN
Department of Materials Science and Engineering, University of Pennsylvania, Philadephia, PA 19104, USA

The morphology of the micro-deformation and fracture processes that occur in the neighbourhood of a notch prior to macroscopic crack growth were determined by a variety of microscopic techniques. The first micro-event that was observed in all instances was the formation of crack-like pores. The shape of the porous zone could not be deduced from existing yield criteria. In thick sections the porous zone transformed to a fibrillated region and in thin films the porous zone tends to transform into a continuous oriented zone. Fibril fracture consisted of a slow process of thinning by shear followed by a rapid rupture. The above micro-events precede macroscopic crack growth in polyethylene.

1. Introduction

Polyethylene is used as thin films for packaging and in thick sections for gas pipes. Failure in these materials involves initiation and growth of a crack. The initiation time may be a large fraction of the total life time of the part. Bragaw [1] showed, for pipe, that one-third of the time to failure is consumed by crack initiation. Therefore, it is important to understand the microscopic events that take place at the root of a notch prior to crack growth.

The long time low stress failure of polyethylene (PE) in thick sections is macroscopically brittle, but microscopically very ductile. Microscopic studies of the long time low stress failure by Lee and Epstein [2] and Chan and Williams [3] have been restricted to scanning electron microscope (SEM) observations of the fracture surfaces. Bandyopadhyay and Brown [4] studied crack propagation in PE and found that the microstructural change in front of the crack was porous, as in a craze. Very little is known about the microscopic events that occur during crack initiation. This paper is an extension of our preliminary studies of crack initiation in polyethylenes [5]. Observations on thick sections correspond to plane strain conditions which occur in engineering structures such as pipes, while the thin film observations are important in their own right as they relate to packaging. However, the observations of both thin and thick sections give a more significant understanding of crack initiation in polyethylene than studying them separately.

In order to study crack initiation, it is necessary to make a notch in the material. It is most important to determine whether the making of the notch with a razor blade, in itself, contributed to the initiation process. Thus, an important part of the experimental work involved the art of making notches so that the least damage was produced. Although a large number of workers on the fracture of polyethylene use a razor blade for making the notch, no information is available in the literature about details of this art. We will describe how it is possible to make a notch in polyethylene so that the damage is insignificant compared to the damage produced by the applied macroscopic loading. In this study it was also found that crack initiation in thin and thick sections has many common features. There are variations which arise primarily from the difference between plane stress and plane strain situations. However, the shape of the deformation zone under plane stress does not conform to the expectation from current theories of yielding.

2. Experimental details

2.1. Material

Observations on thick sections were made on Marlex 6006, a low additive linear blow moulding resin obtained from Phillips Petroleum Company.

0022–2461/84 $03.00 + .12

The density is 964 kg m^{-3}; MFI 0.75; M_w = 130 000 and M_n = 19 600. The specimens were made from 5 mm thick plaques compression moulded in accordance with ASTM 1928 and slow cooled from the melt at about 15° C min^{-1}. The thin films with thicknesses of 0.025 to 0.05 mm were also compression moulded and were generally Marlex 6006. Some thin films of Phillips PE 3408 and DuPont's PE 3406 copolymer piping resin were also used. They have the following characteristics: PE 3408, density 957 kg m^{-3}, MFI 1.5, M_w 250 000 to 300 000 and M_n 15 000 to 20 000; PE 3406, density 942 kg m^{-3} and MFI 0.3.

2.2. Loading methods

The thick specimens were deformed under single edge notched tensile loading in an Instron Machine at a strain rate of 0.05 min^{-1}. The length of the specimen between the grips was 10 mm and its width was 25 mm so that the ratios of specimen thickness to notch depth and specimen width to notch depth were 20 and 100, respectively, to ensure plane strain conditions in the centre of the specimen.

The thin films were deformed in a small jig that was hand-driven and could be accommodated under the optical microscope. The length of the specimen between grips was 20 mm and its width was 7 mm. Double edge notches about 1 mm deep were made in these films.

2.3. Notching and slicing

The notching and slicing were done with a good quality single edge razor blade, 0.2 mm thick with a wedge angle of about 12 degrees, and wedge length of 1 mm. Notching was done at a speed of 0.05 mm min^{-1} for 5 min for thick specimens. The thin ones (0.025 to 0.050 mm thick) were doubly notched under the microscope with a sharp razor blade. The blade was discarded after two notchings. Higher notching speed produced observable deformation. The depth of the notches was less than 0.4 mm to prevent significant damage. Thick specimens were sliced to thicknesses of about 0.25 mm for optical examinations. Slicing speed near the notch was less than 0.5 mm min^{-1}. Good slices were not usually obtained for thicknesses less than about 0.12 mm.

2.4. Microscopic techniques

Various microscopic methods were used: films up to 0.5 mm thick were observed under transmitted and reflected light in a Zeiss microscope using polarizing or Nomarski optics as needed. These films were deformed in a small jig and observed *in situ* so that the dynamic changes could be seen under controlled amounts of strain. After deformation the specimens were cracked open in liquid nitrogen in order to view the deformation zone in a direction perpendicular to the plane of the fracture. These observations were made optically and also with the SEM. Some specimens were etched at room temperature with permanganic acid etchant as described by Bassett and Hodge [6] and observed in the SEM. The various microscopic methods complemented each other to give a multilateral view of the microstructure.

3. Results

The results will be on Marlex 6006 unless stated otherwise.

3.1. Thin films

Fig. 1 shows the development of crack initiation in a 0.05 mm thick film, having a 1 mm notch on either side, with increasing applied strain as observed under transmitted light. In Fig. 1a reversible photoelastic effects are observed; the first indication of a permanent strain is in the form of a black halo (Fig. 1b); the halo grows and within it there develops an oriented zone where the film becomes thinner, depending on the draw ratio. By watching the growth of the triangular deformation zone in Fig. 1c, it is seen that its growth occurs by two processes. (i) There is end growth of the apex where the dark halo grows forward and then orientation occurs within the halo, and the transition from undeformed material to the highly oriented state is gradual as determined by the thickness of the intermediate dark halo. (ii) There is also a side growth of the deformation zone whereby material is converted from the undeformed to oriented state more sharply and rapidly compared to end growth as evidenced by the narrow transition region of the dark halo. Thus, the oriented zone increases in area by simultaneous end and side growth. The increase in the apex angle of the oriented region shows that side growth rate increases more rapidly than end growth.

The next micromechanism that occurs is the splitting of the oriented region (Fig. 1d) where two oriented regions from opposite notches have joined together and eliminated their apex. Fracture

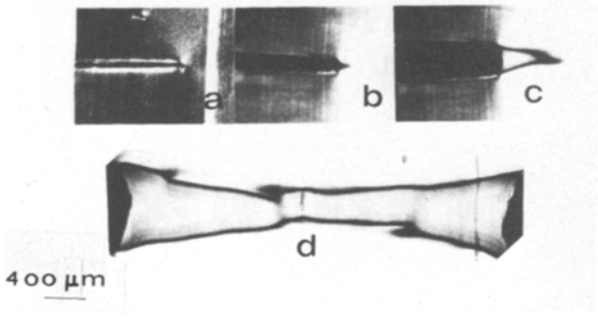

Figure 1 Thin film of Marlex 6006 when deformed at various strains in a small jig showing formation and orientation of a deformed zone. Film thickness ≈ 0.05 mm, notch on each side ≈ 1 mm and a gauge length 10 mm: (a) elastic; (b) porous zone; (c) oriented zone bordered by dark porous zone; and (d) splitting and edge fracture.

has also occurred at the edge of the oriented zone where it borders on the original notch.

Another sequence of crack initiation under increasing strain is shown in Fig. 2 for PE 3408 material. Since this is a black pigmented resin, the contrast under the optical microscope is not as sharp as for the unpigmented Marlex 6006. The first indication of permanent strain was a dark halo. Fig. 2a shows the stage consisting of the outer border which is the dark halo, and the remainder of the material is oriented. The part of the oriented region near the tip forms a continuous film but the remainder has split and fibrillated. These fibrils grow by side growth from unoriented material and at the same time a fibril will continue to draw until it reduces the cross-section to the point of fracture. In Fig. 2b fracture is most evident in the middle of the fibrillated region. Finally, as in Fig. 2c, the fibril fractures at the root of the notch, at which point macroscopic crack growth occurs.

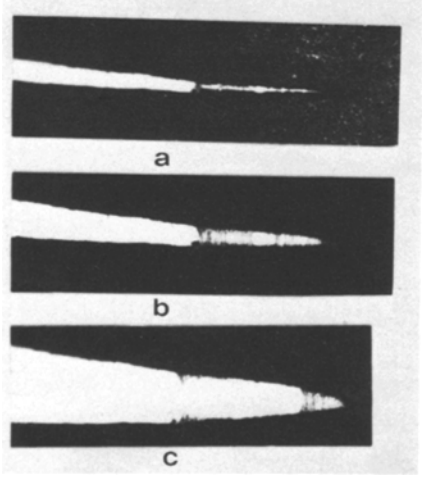

Figure 2 Fibrillation and fibril fracture with increasing strain on a thin film (thickness ≈ 0.05 mm) of PE 3408.

The basic deformation and fracture processes that occur in Figs. 1 and 2 are very much the same. The most evident difference is that Marlex showed a much longer continuous oriented region prior to fibrillation than PE 3408. Under certain conditions such as higher strain rates, the Marlex fibrillates more readily and approaches the behaviour exhibited in Fig. 2.

3.2. The initial stage – the halo

The black halo as seen under transmitted optics is the first evidence of non-elastic deformation. Its nature will now be exhibited. Fig. 3a shows a halo produced in a 0.25 mm thick film under a strain of 5.4%. Fig. 3b shows the same halo after the stress was reduced to zero. The halo diminished somewhat in its vertical dimensions, but its horizontal dimension is approximately the same. When the strain of 5.4% was reapplied, the halo returned to its original size (Fig. 3a). The halo appeared to have a partly reversible component. This behaviour becomes understandable as the porous nature of the dark halo becomes evident.

If the halo consists of pores then it is expected to be dark under transmitted light and lighter than the background under reflected light. Fig. 4 shows a halo that was produced in a thick section and then sliced to a 0.25 mm thick film for observation under the optical microscope. Fig. 4a shows the halo in transmitted light and Fig. 4b under reflected light. The latter is brighter than the background, as expected for a porous material. Since the halo scatters light, the scattering centres will have dimensions which are about the wavelength of light.

Another view of the halo is obtained by adjusting the intensity of the transmitted light so

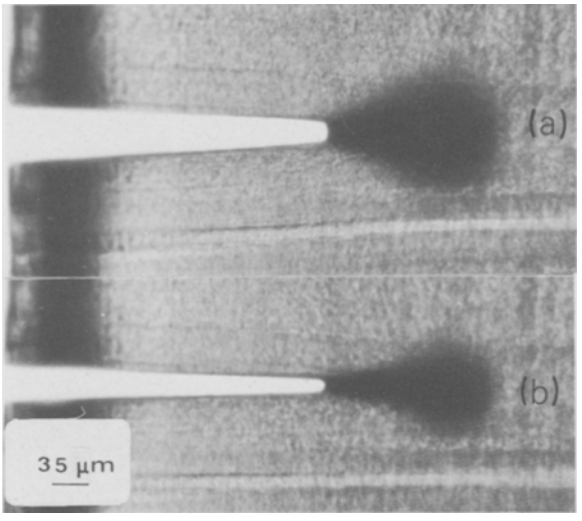

Figure 3 0.25 mm thick film (Marlex 6006) deformed to a strain 5.4% showing (a) under load and (b) unloaded halo.

that contrast effects within the halo become evident. Fig. 5 shows the discontinuous nature of the halo regions. It consists of voids, as will be shown later, whose directionality tends to be crack-like. The term crack-like is used because the pore structure tends to be longer in one direction than in the other and because the long direction tends to be perpendicular to the maximum tensile stress, as for a crack.

The nature of the halo as exhibited by the SEM is shown in the following figures. Whereas the optical view is obtained parallel to the plane of the notch (Fig. 6a), the SEM view (Fig. 6b) is perpendicular to the plane of the notch. The plane of the notch was exposed by fracturing the specimen in liquid nitrogen after the halo was photographed optically in Fig. 6a. In Fig. 6b, region 1–2 is the notch, region 2–3 is highly fibrillated with probably some fibril fracture, region 3–4 is the halo and region 4–5 is virgin material. Fig. 7 shows the higher magnification view of Fig. 6b. The transition between the fibrillated and the porous halo region is rather sharp compared to the gradual diminution in the porosity as the virgin region is approached. Fig. 8a shows the highly oriented and fibrillated region which contains large pores. Fig. 8b shows the gradual decrease in the size of the pores in traversing from the fibrillated zone at the left toward the virgin zone on the right. The pores appear roughly equiaxed from this viewpoint, but from another view of the halo at right angles (Fig. 5) there is a crack-like appearance. The

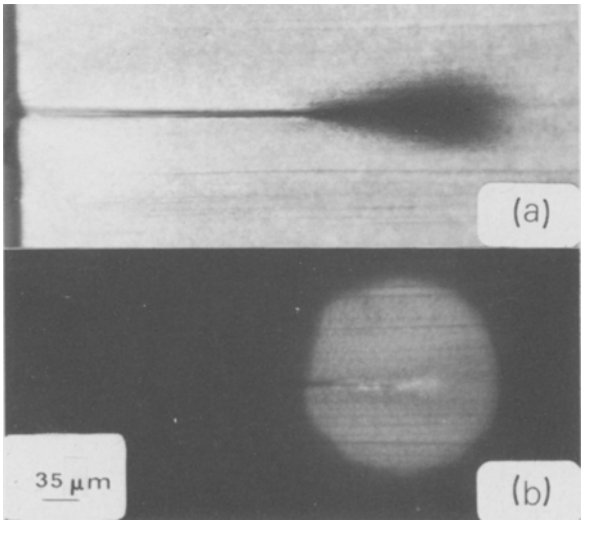

Figure 4 Optical micrographs of a thin slice of Marlex 6006 showing the porous structure of halo in (a) transmitted and (b) reflected light. The thin slice (thickness 0.25 mm) was obtained from a thick specimen which was deformed in plane strain to 22 MPa.

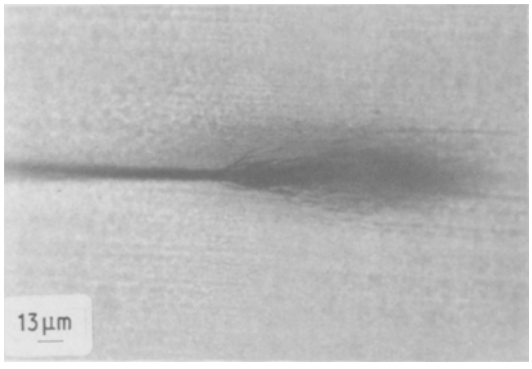

Figure 5 Optical micrograph of a thin slice of Marlex 6006 obtained by slicing from a thick specimen showing crack-like halo structure. The original spectrum was deformed to 18 MPa under plane strain (film thickness 0.25 mm).

apparent differences in structure arise partly from looking at the halo in a different direction, partly from a difference in the magnifications between Fig. 8b and Fig. 5, and partly because SEM shows the topology of the surface whereas Fig. 5 shows the effects of scattering throughout 0.25 mm of material. The virgin material after fracture in liquid nitrogen is shown in Fig. 8c; the appearance of fine pores is present, but this is a result of the fracture process in liquid nitrogen. The halo structure gradually blends into the virgin material, but after looking at many specimens and comparing the length of the halo with the corresponding SEM structure, it is possible to distinguish between deformed and virgin material. In general, the SEM will show evidence of prior deformation which will not be seen optically, simply because SEM has a greater resolution. The halo area consists of a region of increasing porosity as it transforms from the virgin material to the fibrillated and highly oriented state. Even the dark halo region of Fig. 1 is a porous state prior to the formation of the continuous unfibrillated oriented zone.

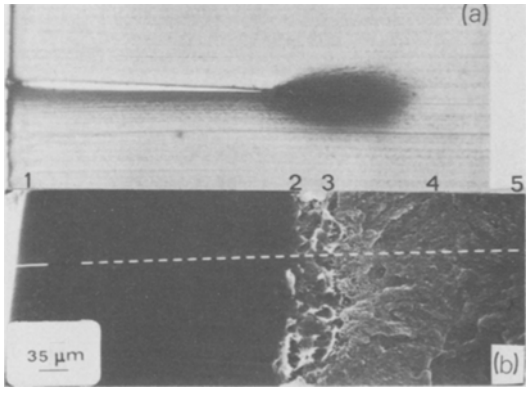

Figure 6 Microstructure of a deformed zone as revealed on a thin slice (thickness 0.25 mm) when viewed in two mutually perpendicular directions. This thin film was obtained by slicing the original specimen that was deformed in plane strain to 19.5 MPa for 5 min: (a) in transmitted light and (b) subsequently fractured in liquid nitrogen and viewed perpendicularly to the fracture surface in SEM; 1–2 notch; 2–3 fibrillated region; 3–4 porous region; 4–5 undeformed matrix (Marlex 6006).

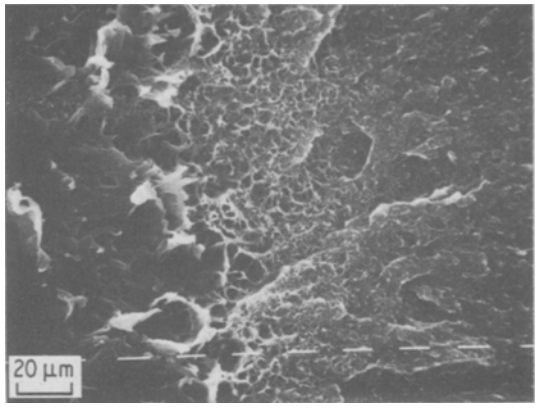

Figure 7 Same as Fig. 6b at higher magnification.

The size of the halo increases with applied stress and time and also depends on thickness. For example, the halo in Fig. 1 is for a 0.05 mm film, and that in Fig. 3 from 0.25 mm film and in Fig. 4 from a thick, plane strain section. Experiments with notched specimens in three-point bending produced very narrow haloes. The shape of the halo is very sensitive to the type of stress distribution around the notch. However, the shapes do not conform to the shapes calculated from prevailing theory using non-Mises or Tresca yield criteria for plane stress and plane strain. The halo could be first observed for a single edge notched specimen under plane strain and a notch depth of 0.25 mm at an applied stress of about 12 MPa compared to the yield point of 24 MPa in 2 min.

3.3. Microstructure revealed by permanganic etch

Bassett and Hodge [6] found that etching polyethylene with permanganic acid nicely reveals the structure of lamellae after making carbon replicas. Olley and Bassett [7] showed that permanganic etching also produces artefacts on the scale of $\approx 10\,\mu m$. It was decided to try permanganic etching of the deformed area around

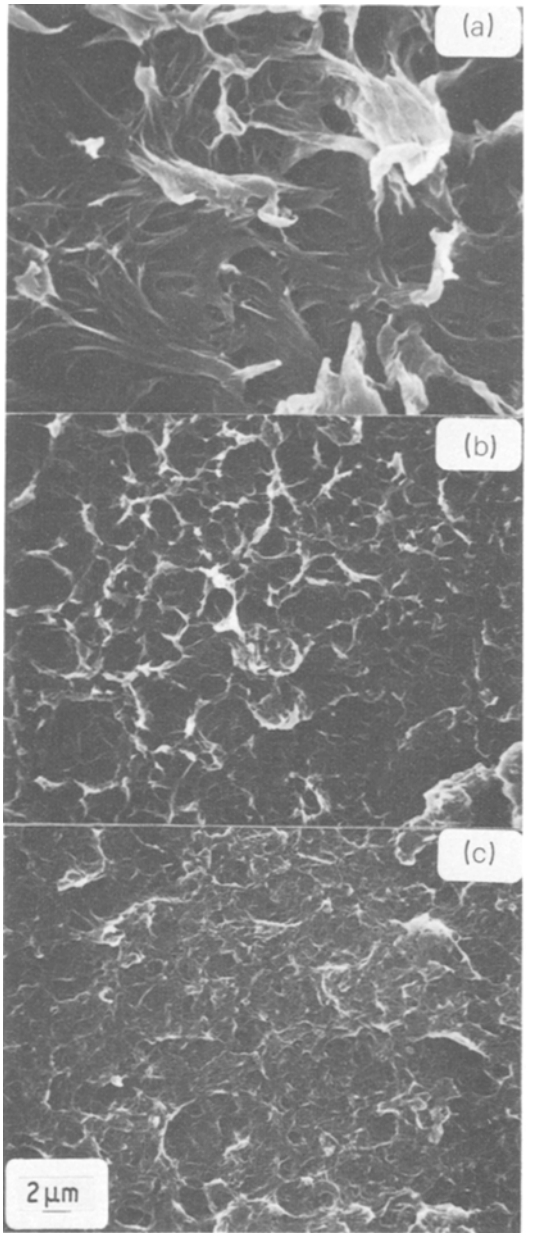

Figure 8 Same as Fig. 6b at higher magnification: (a) fibrillated area; (b) porous zone; and (c) undeformed area.

the notch and to observe the structure with the SEM. The observations were made on the inner surfaces which had been exposed to plane strain deformation and subsequently exposed by slicing with the razor blade.

The optical halo, under transmitted light (Fig. 9a), can be compared with the permanganic etched structure at the same magnification (Fig. 9b) and at a higher one (Fig. 9c). The

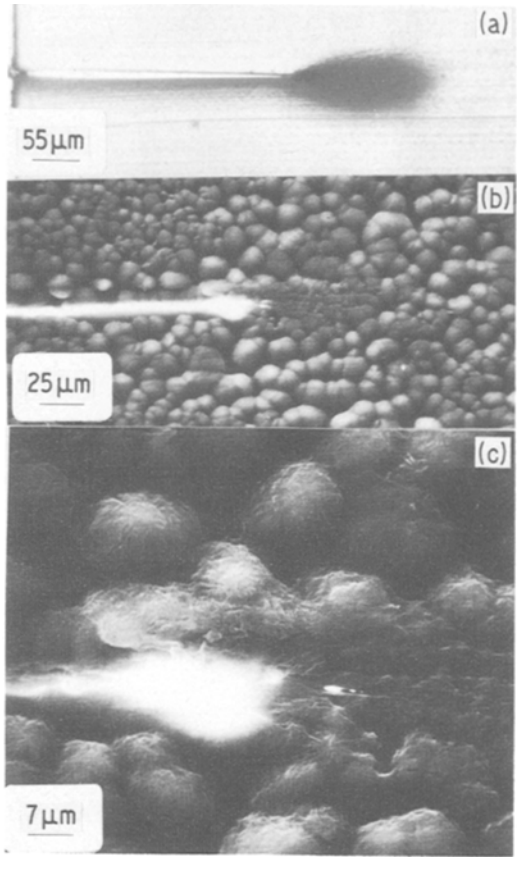

Figure 9 (a) Same as described in Fig. 6a (included for comparison). (b) Same as (a) after permanganic etch for 10 min at 20° C under SEM. (c) Same as (b) at higher magnification.

undeformed background consisting of a spherulite-like structure corresponds to the artefacts reported by Olley and Bassett [7]. The halo structure associated with crack initiation is revealed as a striated porous structure with the striations being on the average perpendicular to the applied tensile stress. The size of the deformed zone as revealed by the permanganic etch is about equal to that of the corresponding optical halo, but appears to be slightly smaller at the lower magnification. The optical contrast is more sensitive at the fringe regions of the halo where the porosity is low because the optical contrast comes from transmitted light which was scattered by 0.25 mm thick material, whereas the SEM reveals only topological features of an etched surface. At high magnifications the permanganic etching seems to be as sensitive as the optical method for revealing the initial formation of the porous structure.

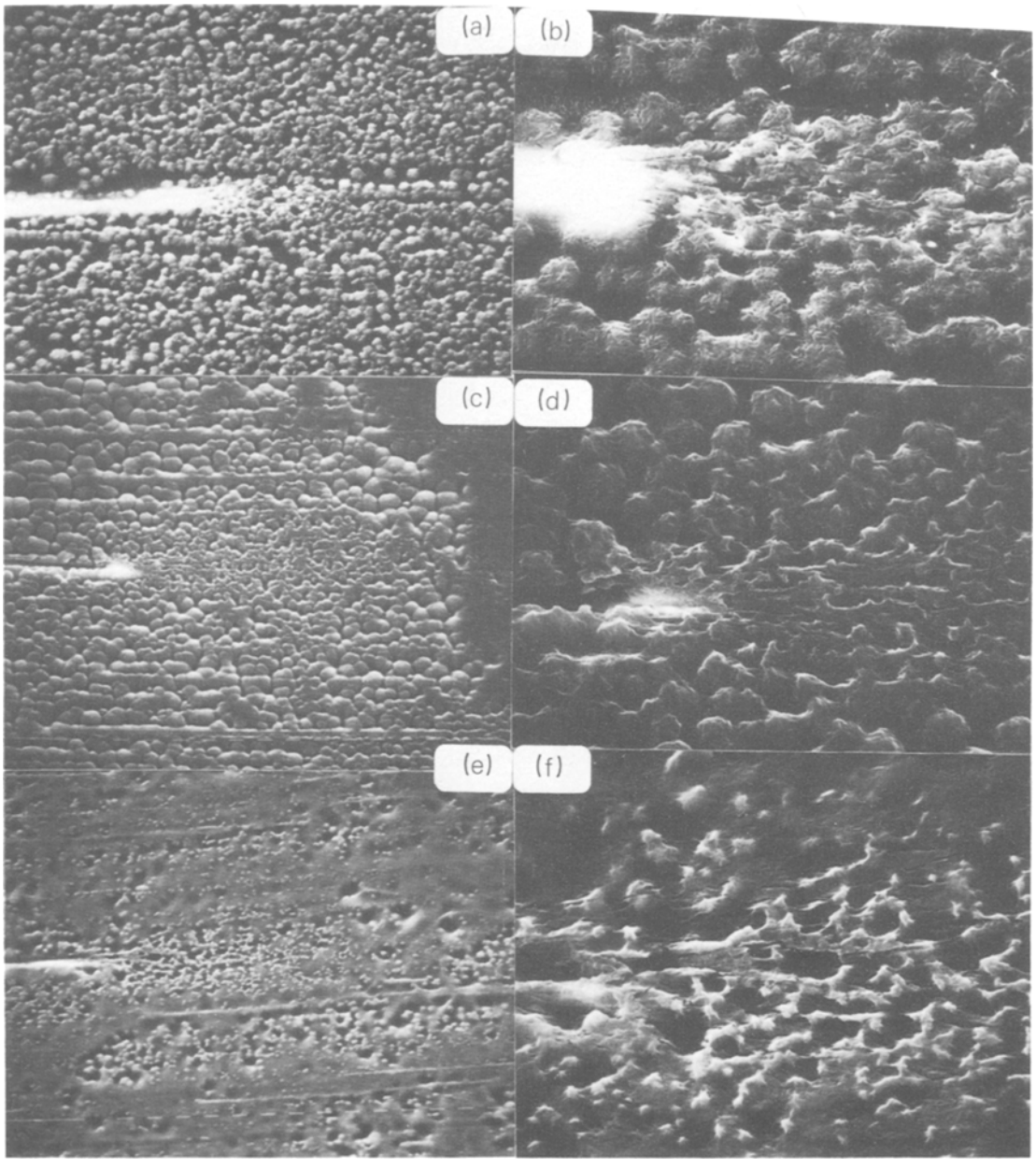

Figure 10 SEMs showing the effects of variations in permanganic etching time on the same deformation zone shown in Fig. 9a: (a) and (b) etched for 2 min; (c) and (d) 15 min; (e) and (f) 30 min; (g) and (h) 60 min; (i) and (j) 90 min; and (k) and (l) 120 min. The spherulitelike regions in undeformed area are artefacts.

Since much of the background structure consists of artefacts it is important to be able to distinguish structure produced by deformation from the undeformed background. A wide variety of artefacts in the undeformed background was produced by varying the etching conditions while keeping the deformed areas the same in that they originated from the same halo (Fig. 6). In Fig. 10, the controlled variable was time. The etchant removed about a few micrometres, depending on time as well as other variables which are not easy to control. At low magnification, the major fraction of the area consists of undeformed material whose artefact structure dominates the

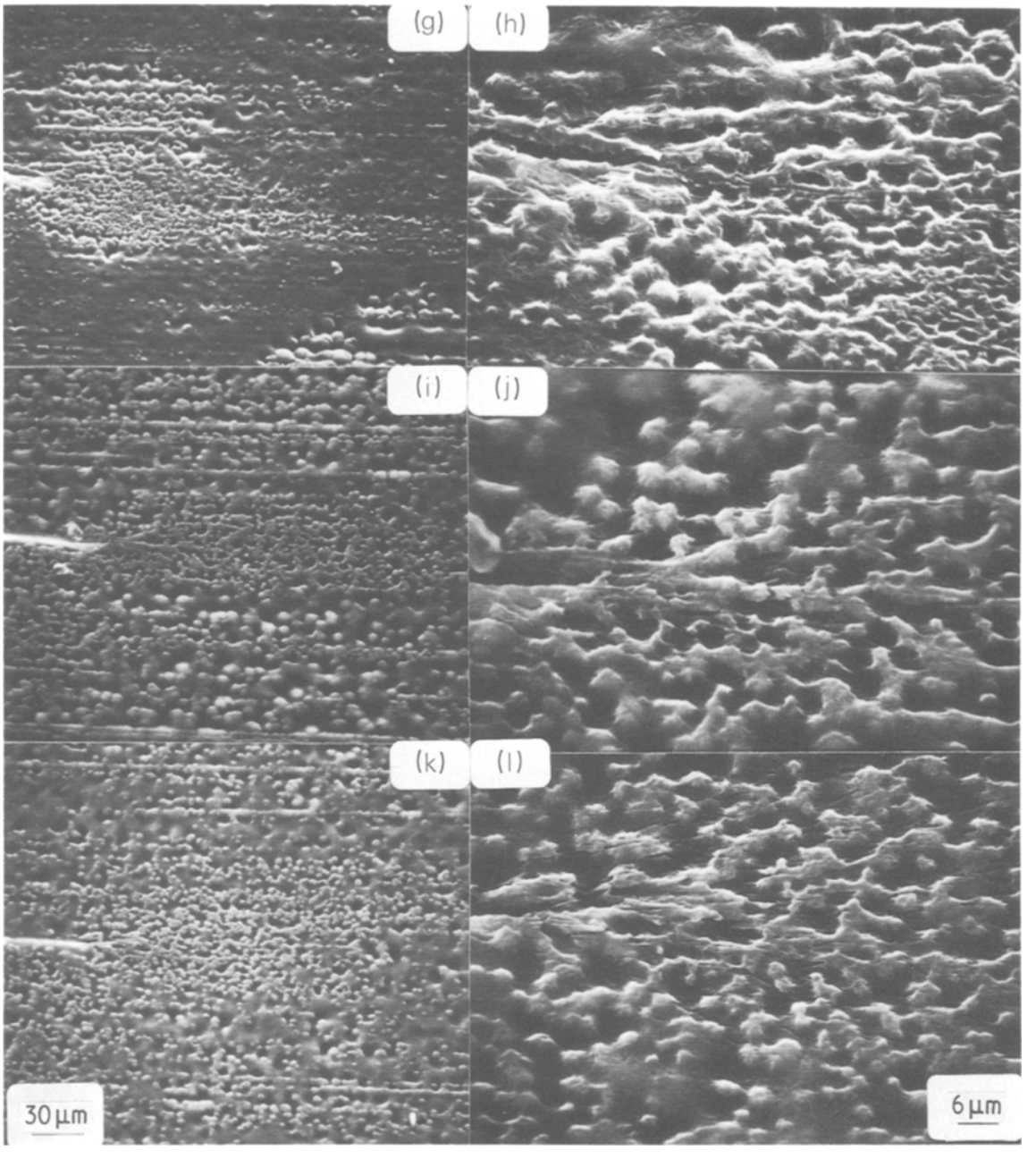

Figure 10 Continued.

micrograph. The deformed zone at low magnification does not stand out against the undeformed as sharply as at high magnification. At high magnification. At high magnification, where the focus is on the deformed region, it is seen that the etched microstructure does not vary appreciably with etching conditions as compared to the views at low magnification. Thus, the deformed region of the halo appears as a striated porous structure which compliments the typical optical halo structure as shown in Fig. 5. Fig. 11 compares the deformed against the undeformed microstructure at higher magnification. The short crack-like nature of the porous zone is again confirmed at the initial stage of crack initiation.

The fibrillation and fibril-fracture states prior to macroscopic crack growth are shown in Fig. 12. More fibrils have fractured away from the notch

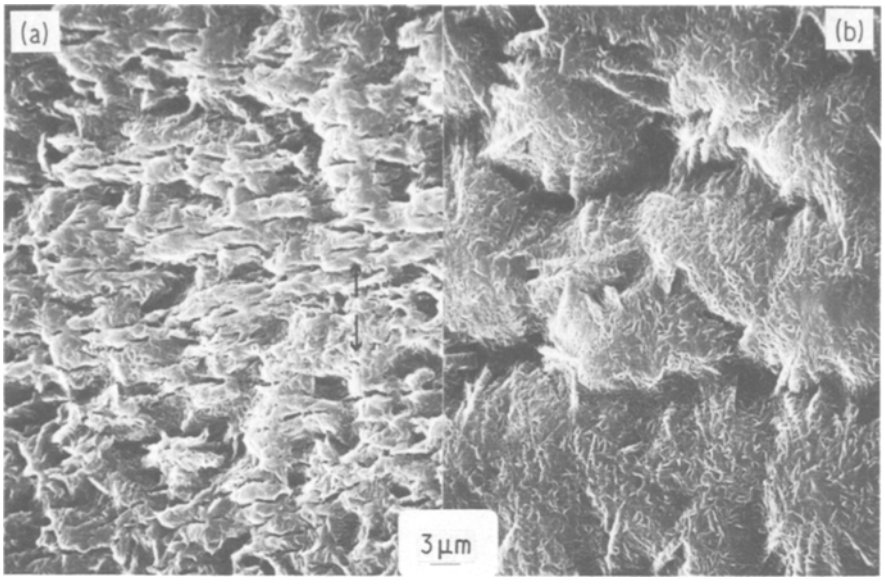

Figure 11 SEM after permanganic etching for about an hour at room temperature: (a) deformed zone, direction of stress is indicated by arrow; and (b) undeformed zone, spherulite-like structures are artefacts (Marlex 6006, plane strain, film thickness 0.25 mm and stress 21.8 MPa).

than at the root of the notch. Complete fracture at the root would constitute macroscopic crack growth. The fibrillated structure is not always so nicely revealed as in Fig. 12 because crack-closure after unloading the specimen tends to obscure the fibrillated structure.

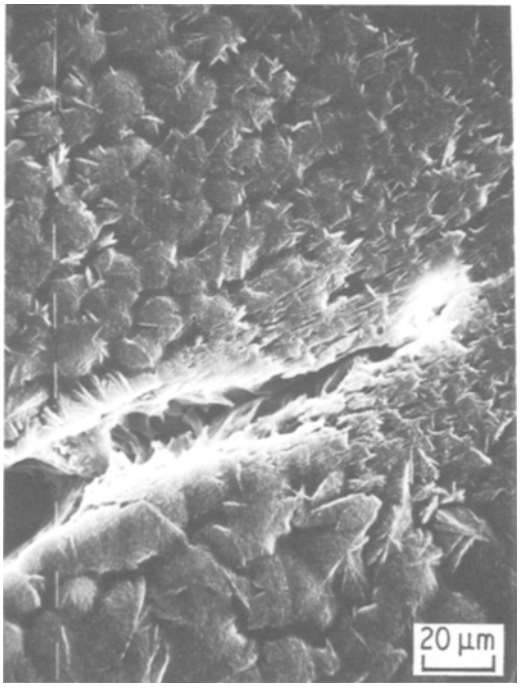

Figure 12 0.25 mm thick slice of the same specimen as Fig. 11 in SEM after permanganic etch showing porous region, fibrillation and fibril fracture.

3.4. Fracture

There are various types of fracture processes if fracture is generally defined as the creation of new surface by means of stress. Forming the porosity of the halo region may be viewed as a micro-fracture event. Figs. 1d and 13 show the fracture of the oriented region by a splitting mechanism. The notch may also be increased in length by an edge fracture of the oriented zone in the absence of fibrillation, as can be seen in Figs. 1d and 13. Then there is a fibril fracture as shown in Figs. 2 and 12.

The details of fibril and edge fracture have both been observed optically in thin films under dynamic conditions and found to occur by the same process. Fig. 14 shows a sequence of events during the fracture of a fibril. While part of a fibril is in the process of thinning, the same fibril may be lengthened by fibril generation at its ends.

The mechanism of fracture that is observed in Fig. 14 will be called shearing fracture. The shearing is most active at the re-entrant corners of a fibril and in the thinner sections. In part, the shearing occurs along highly localized shear planes and in part by a homogeneous shear within the fibril. For example, in Figs. 14c, d and e, there was a highly localized shear along the plane forming

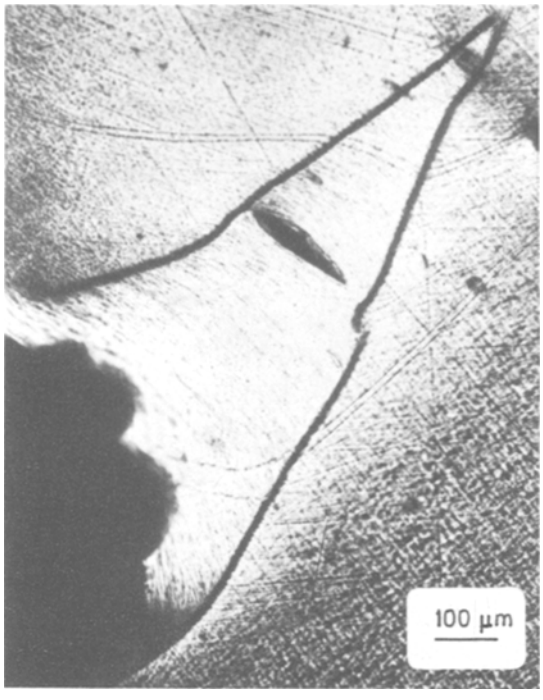

Figure 13 Thin film of PE 3406 (≈ 0.05 mm thick) deformed in a small jig showing the beginning of fibrillation by splitting of the oriented zone and edge fracture. Dark border is the porous zone.

the boundary between the light and dark regions of the fibril and at the same time there was a more homogeneous thinning process throughout the fibril. These observations represent a viewpoint based on dynamic observations under the light microscope. Mechanisms of fracture at the molecular level will be presented in the discussion.

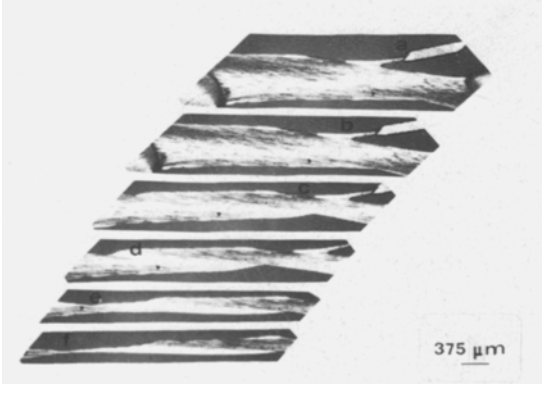

Figure 14 Fracturing of a fibril in plane stress, PE 3406 (film thickness ≈ 0.05 mm). Shearing is most active at the re-entrant corners (the black dot may be taken as a reference point).

4. Discussion

After initiating many deformed zones at notches under various sets of conditions such as plane stress, plane strain, a range of stresses and strain levels, different strain rates, various applied stress fields and with many types of polyethylene, some general conclusions can be made about the nature of crack initiation in PE. By using complementary microscopic techniques and understanding the basic behaviour of macromolecules under stress, the morphological changes during crack initiation become evident. The conclusions are based on notched unoriented PE which was deformed at room temperature in air.

4.1. Sequences of micro-events prior to macroscopic crack growth

The most general observation is that, in all instances, crack initiation begins with the formation of microporosity. The microporosity has the form of an aggregate of microcracks with their long axes tending to be perpendicular to the applied tensile stress.

After the formation of the crack-like micropores there is a general sequence of micro-events whose details depend strongly on the details of the stress field as determined by the thickness of the specimen (plane stress or plane strain). The general sequence of micro-events following pore formation consists of: (i) orientation, (ii) fibrillation or splitting and (iii) film or fibril fracture.

Very thin films (≈ 0.3 mm) tend to form a continuous oriented structure. The oriented film is thinner than the matrix, depending on the local extension ratio. The oriented film grows end-wise and edge-wise as in Fig. 1 and then splits as in Figs. 1d and 13. The film has no apparent porosity and the splitting may be viewed as a first stage in fibrillation. Thick films convert directly from the porous structure to a fibrillated structure. No doubt the transverse stress which exists under plane strain splits the material while it is being oriented so that the continuous oriented film is not produced. The stage which is usually called fracture consists in generating a surface perpendicular to the applied tensile stress. In general, the formation of pores, splitting and fibrillation are also fracture processes with the new surface generated parallel to the applied stress. Macroscopic fracture begins when the fibrils or the edge of the oriented film fracture at the notch.

4.2. The first stage: micro-crack or pore formation

The ductile fracture of solids, and often brittle fracture, proceed by the formation of holes or microcracks prior to the main crack. In the case of metals there are extensive microstructural observations and theoretical calculations concerning pore formation and fracture. One of the earliest microscopic observations was made by Puttick [8]. The extensive microstructural evidence of porosity preceding ductile fracture in metals was recently reviewed by Wilsdorf [9]. An example of a recent general theory of crack propagation by cavitation is given by Wilkinson and Vitek [10].

In the case of polymers Zhurkov and his collaborators [11, 12] by optical techniques showed that the main crack was preceded by microscopic cracks of the type observed in this investigation. Zhurkov's work was reviewed by Bartenev and Zuyev [13]. Hannon [14] presented microscopic observations of void formation during the brittle fracture of polyethylene and also gave a brief review of many experimental and theoretical investigations which involved the formation of microcavities prior to fracture in polymers. Kambour [15] and Kramer [16] reviews of crazing also emphasized that pore nucleation precedes fibrillation. Bandyopadhyay and Brown [4] showed porosity preceded crack growth in PE.

There is no doubt that void formation precedes fibrillation. However, the microcracks or voids do not necessarily produce fibrillation, as evidenced by the formation of a continuous oriented film in Figs. 1 and 13. There are many views concerning the nucleation of a void in amorphous polymers. Wellinghoff and Baer [17] found that strain localization was the first evidence of non-elastic deformation in films stretched in the transmission electron microscope (TEM). Brown and Ward [18] showed that polymers generally undergo an intrinsic softening during yielding which probably is caused by pore formation. Kramer [16] postulated that the intrinsic softening leads to strain localization and subsequent voids. Kambour [15] suggested that there are weak points in the polymer which are opened by the hydrostatic stress. In Argon's theory of craze nucleation [19], it was assumed that the stress produces a shear patch which when blocked leads to the formation of a pore. The details of pore formation at the 0.1 to 10 nm level of resolution are speculative. However, at the micrometre level, crazes start at dirt particles (Kramer [16]). Haas and MacRae [20] optically observed that in thin films of biaxially stressed PE most voids started at the centre of spherulite boundaries. These voids formed microcracks which usually grew in a radial direction in the spherulite. It is generally thought that there is a heterogeneity at the centre of spherulites which causes them to nucleate. A general statement will now be made with respect to the formation of voids in polymers.

It is our view that generally an isotropic, non-crosslinked polymer will form voids in a stress field which produces the oriented state. The geometrical rearrangement from the isotropic to the oriented state requires an unpacking that produces voids. The voids may not persist into the oriented state (Figs. 1 and 13). The voids may coalesce and produce the state of fibrillation called crazing. It appears impossible to produce fibrillation without first producing voids. Voiding is a necessary geometric precursor to fibrillation. However, all voiding does not necessarily lead to fibrillation as shown in Figs. 1 and 13. In this case the voids disappeared, but a subsequent void occurs in the form of a split (Fig. 1d). Thus, the voids may be a transient phenomenon which was enhanced by the increase in the hydrostatic tension component of the stress at the neck formed between the unoriented and oriented regions of the film.

An indication that the microvoid formation may be reversible is seen in Fig. 3, where the halo decreased in size when the stress was relaxed. No doubt the shrinkage of the voids is caused by the surface tension at the inner surface of the voids combined with the reduction in stress when the applied load is removed and the shrinkage of the oriented polymer surrounding the void.

A more sophisticated viewpoint of microvoid formation should be taken. It is suggested that during the formation of microvoids, orientation of the surrounding polymer takes place at the same time. The orientation effect is not easily observed in the early stage because the scattering from the microvoids may be overwhelming. After the microvoids disappear, the orientation of the fibrils or the continuous film becomes observable. Finally, all voids disappeared, as in the oriented region of Figs. 1c, d and 13, or they may have coalesced to form the gross porosity that occurs between fibrils. It is not certain that the concept of meniscus instability [16, 22] that has been used for craze growth adequately describes the transition

from the porous to the fibrillated state in the case of polyethylene.

4.3. Fibrillation

The fibrillation that is observed in PE (Figs. 2, 8 and 12), and by Lee and Epstein [2] and Chan and Williams [3], is coarse compared to the ≈ 20 nm diameter fibrils that are observed in crazes in other polymers [15, 16]. Also, the thickness of the fibrillated zone is large compared to the 0.1 to 1.0 μm thickness of most crazes. Probably these fibrillated structures should be called coarse crazes. It is possible to form thin crazes in PE by exposure to an environmental agent such as nitrogen or isopentane at low temperatures, as shown by Kamei and Brown [21].

Whether PE transforms from the microvoid structure to the continuous oriented film or to the fibrillated structure depend primarily on the stress field. For plane stress conditions, the continuous oriented films may be produced; under plane strain as in a thick section, fibrillation is always produced by the tensile stress transverse to the direction of orientation.

It was observed that increasing the rate of loading in thin films would enhance the formation of fibrillation *vis-à-vis* the formation of the continuous oriented film. That a high rate of loading favours fibrillation over the formation of a deformation zone is contrary to the suggestion by Kramer [16]. Kramer suggested that the ease of fibrillation in amorphous polymers increased as the degree of entanglement decreased. Kramer's reasoning was based on the idea that the greater the degree of entanglement the higher the stress required to disentangle, as required for fibrillation. Our observation that increased strain rate increases the tendency to fibrillate may be explained by the increase in stress required for the higher strain rate and this increase in stress more than compensates for the increase resistance against fibrillation. If the fibrillation process occurred exclusively by the unslipping of the points of entanglement, then the fibrillation processes might be more difficult at the higher strain rate in spite of the increase in stress. However, if chain scission and disentanglement both occurred during fibrillation, as also suggested by Kramer [16], then the kinetics of the scission mechanism would be more responsive to an increase in stress and not as dependent on strain rate as for the disentanglement mechanism. Also, the coarse fibrillation process in a crystalline polymer is, most likely, different from the fine fibrillation that occurs during the crazing of an amorphous polymer.

One may also view the fibrillation process as the coalescence of the microvoids into the gross porosity associated with the fibrillated state. There must exist a critical condition as to whether the microvoids will shrink so that a continuous oriented film forms or whether they will coalesce and form splits or fibrillation. The key factors are the transverse stress, the ease of disentanglement or possible chain scission and void mobility.

4.4. Fibril fracture

Fibril fracture was observed dynamically, as shown in Fig. 14. The fracture process consists of a slow phase where the fibril thins by shear and a final rapid fracture. Fig. 15 is a schematic of the processes; localized shearing occurs along a plane such as AB and also homogeneous shearing occurs in parts of the fibril above and below AB. When the fibril reaches a critical cross-section it fractures rapidly. This critical cross-section depends on the stress. If the fibril is being drawn more rapidly so that the stress is higher, then sudden fracture occurs at a greater cross-section area. These observations are consistent with the observations of the fractured surface by Chan and Williams [3] that faster crack growth produced fibrils with a larger cross-section.

At the molecular level, the shear thinning process could occur by chain disentanglement and/or chain scission. Probably chain disentanglement dominates at the slow shear rates. The sudden final fracture process probably involves primarily chain scission.

4.5. Shape of the halo

The shapes of the haloes (Figs. 2b, 3 to 6 and 9 and 10) do not agree with the shapes expected for a Tesca or von-Mises yield criterion even when the yield criterion is modified by the hydrostatic component of the stress. Our porous zone is more concentrated along the plane of the crack where the shear stress is zero. The shape of the halo indicates that the Tresca or von-Mises shear yield criterion, even when modified by the hydrostatic component of the stress, is not applicable to a yield process associated with the initiation of the microcavities. There do not exist data for the macroscopic yield criterion for PE in the combined stress domain where the principle stresses

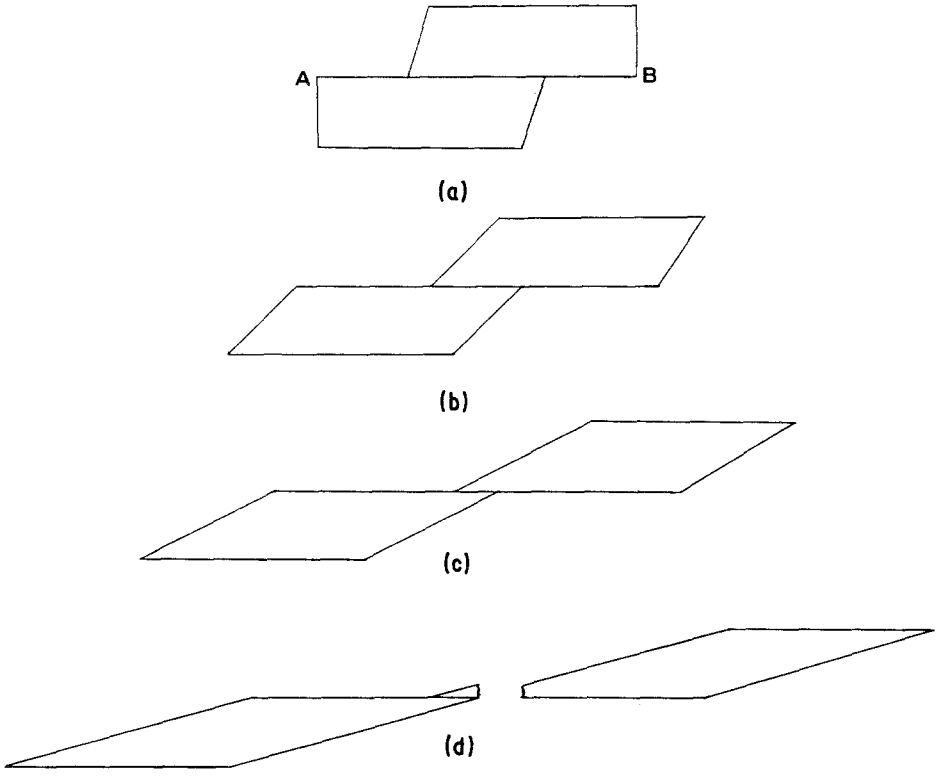

Figure 15 Schematic of the shearing off process as exhibited in Fig. 14.

are positive. Since initiation of plastic deformation is associated with microcavitation, possibly a maximum tensile stress combined with the hydrostatic tension may be the more appropriate basis for the yield criterion. A detailed micromechanics analysis based on the observed microdeformation mechanisms and the shapes of the halo may be required to deduce the yield criterion which is applicable to the initiation of porosity in polyethylene.

5. Summary

(a) Macroscopic crack initiation in PE under plane strain consists of the following sequence of micro-events: (i) generation of porosity, (ii) increase in size of pores, (iii) fibrillation and (iv) fibril fracture.

(b) For crack initiation under plane stress the sequence may be modified as follows: (i) generation of pores, (ii) formation of a continuous oriented film, (iii) splitting and edge fracture near the notch.

(c) The porous zone consists of crack-like pores which tend to be perpendicular to the applied tensile stress.

(d) The fracture of fibrils occurs by two processes, a slow shear thinning followed by rapid rupture.

(e) The shape of the porous zone cannot be predicted by the existing yield criteria.

Acknowledgement

Financial support by the Gas Research Institute is gratefully acknowledged. Support was also received from NSF through the use of the Central Research Facilities in the MRL program. Very helpful discussions were provided by Professor J. L. Bassani and Mr L. Fager of the Mechanical Engineering Department. SKB is particularly grateful to Ms D. Ricketts for her assistance in SEM.

References

1. C. G. BRAGAW, Proceedings of the 6th Plastic Pipe Symposium, April 1978 (American Gas Association, Arlington, VA, 1978) p. 36.
2. C. S. LEE and M. M. EPSTEIN, *Polym. Eng. Sci.* **22** (1982) 549.
3. M. K. V. CHAN and J. G. WILLIAMS, *Polymer* **24** (1983) 234.
4. S. BANDYOPADHYAY and H. R. BROWN, International Conference on Materials 3, 1979 (Pergamon Press, New York, 1980).
5. N. BROWN and S. K. BHATTACHARYA, Proceed-

ings of the 8th Plastic Fuel Gas Pipe Symp., New Orleans, 29 November–1 December 1983 (American Gas Association, Arlington, VA, 1983) p. 58.
6. D. C. BASSETT and A. M. HODGE, *Proc. Roy. Soc. London.* **A377** (1981) 25.
7. R. H. OLLEY and D. C. BASSETT, *Polymer* **23** (1982) 1707.
8. K. E. PUTTICK, *Phil. Mag.* **4** (1959) 964.
9. H. G. F. WILSDORF, *Mater. Sci. Eng.* **59** (1983) 1.
10. D. S. WILKINSON and V. VITEK, *Acta Metall.* **30** (1982) 1729.
11. S. N. ZHURKOV, V. A. MARIKHIN and A. I. SLUTSKEN, *FTT* **1** (1959) 1159.
12. *Idem, ibid.* **1** (1959) 1759.
13. G. M. BARTENEV and Y. S. ZUYEV, "Strength and Failure of Visco-Elastic Materials" (Pergamon Press, London, 1968) p. 15.
14. M. J. HANNON, *J. Appl. Polym. Sci.* **18** (1974) 3761.
15. R. P. KAMBOUR, *Macromol. Revs.* **7** (1973) 1.
16. E. J. KRAMER, "Advances in Polymer Science", Vol. 50, "Crazing", edited by H. H. Kausch, (Springer-Verlag, Berlin, 1983) Chap. 1.
17. S. WELLINGHOFF and E. BAER, *J. Macromol. Sci., Phys.*, **B11** (1975) 367.
18. N. BROWN and I. M. WARD, *J. Polym. Sci.* **6** (1968) 607.
19. A. S. ARGON, *J. Macromol. Sci., Phys.* **8** (1973) 573.
20. T. W. HAAS and P. H. MacRAE, SPE RETEC, Washington, DC, September (1967).
21. E. KAMEI and N. BROWN, *J. Polym. Sci. Polym. Phys. Ed.* in press.
22. A. S. ARGON and J. G. HANNOOSH, *Phil. Mag.* **36** (1977) 1195.

Received 10 October
and accepted 26 October 1983